Correlated Calcium Uptake and Release by Mitochondria and Endoplasmic Reticulum of CA3 Hippocampal Dendrites after Afferent Synaptic Stimulation

Natalia B. Pivovarova,[1]* Lucas D. Pozzo-Miller,[2,3]* Jarin Hongpaisan,[1] and S. Brian Andrews[1,3]

[1]Laboratory of Neurobiology, National Institute of Neurological Disorders and Stroke, National Institutes of Health, Bethesda, Maryland 20892-4062, [2]Department of Neurobiology and Civitan International Research Center, University of Alabama at Birmingham, Birmingham, Alabama 35294-0021, and [3]The Marine Biological Laboratory, Woods Hole, Massachusetts 02543

Mitochondria and endoplasmic reticulum (ER) are important modulators of intracellular calcium signaling pathways, but the role of these organelles in shaping synaptic calcium transients in dendrites of pyramidal neurons remains speculative. We have measured directly the concentrations of total Ca (bound plus free) within intracellular compartments of proximal dendrites of CA3 hippocampal neurons at times after synaptic stimulation corresponding to the peak of the cytoplasmic free Ca^{2+} transient (1 sec), to just after its decay (30 sec), and to well after its return to prestimulus levels (180 sec). Electron probe microanalysis of cryosections from rapidly frozen slice cultures has revealed that afferent mossy fiber stimulation evokes large, rapid elevations in the concentration of total mitochondrial Ca ($[Ca]_{mito}$) in depolarized dendrites. A single tetanus (50 Hz/1 sec) elevated $[Ca]_{mito}$ more than fivefold above characteristically low basal levels within 1 sec of stimulation and >10-fold by 30 sec after stimulation. This strong Ca accumulation was reversible, because $[Ca]_{mito}$ had recovered by 180 sec after the tetanus. Ca sequestered within mitochondria was localized to small inclusions that were distributed heterogeneously within, and probably among, individual mitochondria. By 30 sec after stimulation an active subpopulation of ER cisterns had accumulated more Ca than had mitochondria despite a ~1 sec delay before the onset of accumulation. Active ER cisterns retained their Ca load much longer (>3 min) than mitochondria. The complementary time courses of mitochondrial versus ER Ca^{2+} uptake and release suggest that these organelles participate in a choreographed interplay, each shaping dendritic Ca^{2+} signals within characteristic regimes of cytosolic Ca^{2+} concentration and time.

Key words: calcium; endoplasmic reticulum; mitochondria; hippocampus; synaptic activity; electron probe x-ray microanalysis

Mitochondria and the endoplasmic reticulum (ER) are the main organellar components of a cellular calcium regulatory system that is essential for shaping intracellular calcium signals. Although the importance of the ER has been recognized for decades (for review, see Berridge, 1998; Meldolesi, 2001), our understanding of the role of mitochondrial Ca^{2+} transport recently has undergone considerable evolution (Friel, 2000; Pozzan and Rizzuto, 2000). There is now accumulating evidence that in a variety of cell types, including neurons, elevation of the free cytosolic Ca^{2+} concentration ($[Ca^{2+}]_i$) leads to mitochondrial Ca^{2+} uptake and that this has a major impact on Ca^{2+} signaling (Babcock and Hille, 1998; Duchen, 1999; Pozzan and Rizzuto, 2000). Thus, somatic mitochondria in several neuronal cell types buffer physiological calcium loads elicited by depolarization and/or action potentials (Thayer and Miller, 1990; Friel and Tsien, 1994; White and Reynolds, 1995; Herrington et al., 1996; Babcock et al., 1997). Under pathological conditions, e.g., excessive glutamate exposure, mitochondria of CNS neurons accumulate large amounts of Ca (Budd and Nicholls, 1996; Stout et al., 1998; Brocard et al., 2001), ultimately leading to mitochondrial dysfunction and cell death (Reynolds, 1999; Nicholls and Budd, 2000).

Regarding synaptic Ca^{2+} transients, mitochondrial Ca^{2+} transport contributes to the regulation of $[Ca^{2+}]_i$ in presynaptic terminals during normal transmission (David et al., 1998; Peng, 1998) and post-tetanic potentiation [Tang and Zucker (1997), but see Zenisek and Matthews (2000)]. To date, however, the role of mitochondria in modulating spatiotemporal patterns of synaptically evoked postsynaptic Ca^{2+} transients, for example in dendrites of CNS pyramidal neurons, is unclear. Yet dendritic mitochondria are potentially of great importance because, given the subcellular architecture of dendrites, they are exposed to substantial $[Ca^{2+}]_i$ elevations after synaptic activity (Petrozzino et al., 1995; Helmchen et al., 1996).

In a previous study we found no elevation of mitochondrial total Ca concentration ($[Ca]_{mito}$) in hippocampal CA3 pyramidal dendrites at 3 min after synaptic stimulation, although a subset of ER contained large amounts of Ca at this and even later times (Pozzo-Miller et al., 1997). These results revealed a remarkably long persistence for ER Ca sequestration but did not address the subcellular distribution of Ca at times close to synaptically driven $[Ca^{2+}]_i$ transients, which peak and decay within seconds of synaptic stimulation (Regehr et al., 1989; Jaffe et al., 1992; Magee et al., 1995; Petrozzino et al., 1995; Spruston et al., 1995). We now have determined the distribution of Ca within the ER and mito-

Received July 15, 2002; revised Sept. 19, 2002; accepted Oct. 1, 2002.

This work was supported by the National Institutes of Health Intramural Research Program. We thank Drs. C. A. Brantner, R. D. Leapman, and T. S. Reese for resource support, helpful discussions, and technical assistance.

*N.B.P. and L.D.P.-M. contributed equally to this work.

Correspondence should be addressed to Brian Andrews, Building 36, Room 2A-21, Laboratory of Neurobiology, National Institute of Neurological Disorders and Stroke, National Institutes of Health, 36 Convent Drive, Bethesda, MD 20892-4062. E-mail: sba@helix.nih.gov.

 0270-6474/02/2210653-09$15.00/0

chondria of proximal CA3 dendrites at the peak of the free Ca^{2+} transient (1 sec), just after its decay (30 sec), and well after its return to prestimulus levels (180 sec). A large rise and fall of $[Ca]_{mito}$ was observed during the first minutes after synaptic activity in parallel with a delayed but sustained Ca accumulation in a subset of ER. These results indicate that in pyramidal dendrites both ER and mitochondria reversibly accumulate Ca but with characteristically different sequestration mechanisms and complementary temporal properties that are likely to be important in the modulation of dendritic Ca^{2+} signals.

MATERIALS AND METHODS

Stimulation and rapid freezing of organotypic hippocampal slice cultures. Slice cultures of hippocampus were prepared from postnatal day 7 rats in the manner of Stoppini et al. (1991). Such organotypic slice cultures are widely accepted experimental models (for review, see Gähwiler et al., 1997) and are essential for the present experiments because they provide healthy superficial neuronal cell bodies, dendrites, and synapses that are close enough to the surface to allow for rapid freezing with excellent structural preservation (Pozzo-Miller et al., 1993) and no elemental redistribution. The specific experimental setup is essentially similar to that described and schematically diagrammed in Pozzo-Miller et al. (1997), with one significant modification: two insulated nichrome wires (20 μm in diameter; California Fine Wire, Grover Beach, CA) for afferent fiber stimulation were attached permanently to custom-modified 12 mm Millicell-CM filter inserts (Millipore, Bedford, MA). The slice grew above one exposed uninsulated section of the wire that was fixed flush against the filter insert membrane, such that the wire ran under the dentate gyrus. The presence of the wires had no discernible effect on the growth, anatomy, or synaptic circuitry of the cultures. Just before a slice was transferred to a recording chamber, the exposed uninsulated section of the second wire was lowered onto the slice parallel to the lower wire, with a spacing of ~1 mm, and was fixed to the edge of the insert with silicone vacuum grease. The recording chamber was perfused continuously with oxygenated artificial CSF (aCSF) containing (in mM) 124 NaCl, 2 KCl, 1.24 KH_2PO_4, 1.3 $MgSO_4$, 17.6 $NaHCO_3$, 2.5 $CaCl_2$, and 10 D-glucose; the solution was bubbled with 95% O_2/5% CO_2. Field EPSPs (fEPSPs) were evoked at low frequency by single pulses (100 μsec duration) delivered to the top wire by a multichannel stimulator and isolator set-up (Master-8 and ISO-Flex, AMPI, Jerusalem, Israel) and were recorded with a bridge amplifier (Axoclamp-1A, Foster City, CA), using an extracellular glass microelectrode filled with aCSF (2 MΩ final resistance) positioned in CA3 stratum lucidum. This arrangement was effective for generating fEPSPs along the apical CA3 dendritic field and permitted selection of the stimulus strength that was necessary to evoke subthreshold fEPSPs (~0.5 mV, without superimposed population spike) in each culture individually.

For slices with a 1 sec interval between stimulation and freezing, cultures with the wires still in position were positioned briefly under a dissecting microscope to wick off adventitious surface fluid and to place (with a fine needle) three delicate copier toner marks that later would be used to triangulate the CA3 region in frozen specimens. Cultures then were mounted on custom-made freezing stages that adapted the Millicell-CM inserts to a custom-modified rapid freezing machine (Life-Cell CF-100; The Woodlands, TX). These steps required ~10 sec; in no case was the tissue touched or otherwise disturbed. The stimulator was used to trigger the freezing machine as well as the stimulus train, allowing rapid freezing at accurately programmable intervals as short as a few milliseconds between the delivery of a stimulus to mossy fibers and the instant of impact on the freezing block. The stimulus train used here, 50 Hz/1 sec, is a standard high-frequency train and is identical to that described as the "single train" in previous work (Pozzo-Miller et al., 1997). For 30 sec (and longer) experiments the interval is long enough that cultures can be stimulated alternatively in the recording chamber (and therefore can use cultures grown with or without embedded stimulating wires) and then mounted on stages and rapidly frozen. Experiments were performed to evaluate all permutations, and no differences were found among the various procedures. Controls, i.e., nonstimulated cultures, were subjected to all experimental manipulations except delivery of the tetanus. Again, no differences were observed between controls frozen directly from the recording chamber and those premounted on freezing stages.

Experiments were performed on slices 6–8 d *in vitro*. This relatively short time avoids one disadvantage of slice cultures, namely, that aberrant sprouting by intrinsic fibers may occupy vacant postsynaptic sites, leading to hyperexcitable slices. This isolation-induced sprouting becomes a significant problem only after 2 weeks *in vitro* (Pozzo-Miller et al., 1994).

Analytical electron microscopy. The principles and techniques for cryosectioning, electron microscopy, and electron probe x-ray microanalysis (EPMA) for measuring total (free plus bound) concentrations of diffusible elements at the subcellular level are well established (Kitazawa et al., 1983; Somlyo, 1985) (for review, see Roomans and Von Euler, 1996; Meldolesi and Grohovaz, 2001). Techniques for cryosectioning and EPMA within organelles of pyramidal neurons in slice cultures are described in Pozzo-Miller et al. (1997). Briefly, cryosections (80 nm nominal thickness) were prepared from the well frozen specimen face by means of a Leica Ultracut S/FCS ultracryomicrotome (Deerfield, IL). Sections were mounted on carbon- and Formvar-coated grids and cryotransferred into an EM912 Omega electron microscope (LEO Electron Microscopy, Thornwood, NY) equipped with a Linksystem Pentafet energy-dispersive x-ray (EDX) detector (Oxford Instruments, Concord, MA) and a ProScan HSSC-1 slow-scan CCD camera (1024 × 1024) interfaced to AnalySIS software (Soft-Imaging Software GmbH, Munster, Germany). Sections were freeze dried in the microscope at approximately –100°C and then recooled to approximately –170°C for imaging and x-ray analysis. Individual x-ray spectra were recorded for 100 sec at ~4 nA probe current, using a focused probe with a diameter of 100 nm for mitochondria and cytoplasm and ≤50 nm for ER cisterns.

Spectra subsequently were processed and quantified using the program DeskTop Spectrum Analyzer (DTSA) for the Macintosh [C. E. Fiori, C. R. Swyt, R. L. Myklebust (1993) Office of Standard Reference Data, National Institute of Standards and Technology, Gaithersburg, MD]. A simplex fitting routine and the peak/continuum method (Kitazawa et al., 1983) were used to quantify the concentrations of the following elements in units of mmol/kg dry weight: Na, Mg, P, Cl, K, and Ca. Methods for converting concentrations to mmol/kg wet weight (the units for data presentation in Figs. 2*B*, 4) are described by Roomans and Von Euler (1996) and by Pozzo-Miller et al. (2000). Relative dry mass fractions required for this calculation were derived from x-ray continuum counts (Buchanan et al., 1993) specifically from these experiments. Mass fractions were 0.15 ± 0.02, 0.27 ± 0.02, and 0.45 ± 0.03 for cytoplasm, ER, and mitochondria, respectively; they were distributed normally and are consistent with published data (Pozzo-Miller et al., 1997, 2000). Throughout this work elemental symbols with the oxidation state specified, e.g., Ca^{2+}, are used conventionally to indicate ions in the free, water-solvated state, whereas symbols without such specification, e.g., Ca, refer to the element without regard to whether it is free or bound and are used mainly to indicate total concentrations as measured by EPMA.

Sampling, data analysis, and statistics. Individual x-ray spectra were recorded from the major Ca^{2+}-regulating compartments of CA3 pyramidal dendrites, namely, cytoplasm, mitochondria, and ER. The term "ER" is used by convention throughout this paper to refer to structurally identified smooth-membrane cisterns and may include some elements that were not in fact a part of the true ER network, e.g., endocytic vesicles; this is, however, unlikely at the locations that were analyzed and would not affect materially any conclusions, as further discussed in Results. Measurements were performed at a distance of 50–100 μm from the cell soma and therefore were from unbranched primary dendrites, each arising from a different cell. Duplicate sampling, i.e., two dendrites from the same cell or two measurements from the same dendrite, was not likely. The afferent stimulation used here depolarizes most, but not all, CA3 neurons in a culture and most, but not all, dendrites of a given neuron. Because the aim of the present experiments was to compare Ca^{2+} buffering in various dendritic compartments after Ca^{2+} influx, dendrites that did not respond to the stimulus train [that is, dendrites that did not show the characteristic elemental changes known to accompany dendritic depolarization and Ca^{2+} influx and in which the elemental composition of all compartments was statistically (ANOVA) indistinguishable from controls] were excluded from the data set. Typically, the fraction of dendrites that was excluded was small, ~10%.

Our sampling strategy aimed to acquire five analyses per dendrite for each compartment from five different stimulated dendrites per culture. In practice, the actual number of analyses per section varied because of an abundance or paucity of organelles or dendrites but in no case was fewer than three compartments or dendrites. The final data set was unbalanced and was treated as such for statistical analysis. Nested ANOVA indicated that in all cases there were no differences between slice cultures from the

Table 1. Elemental concentrations in dendritic compartments of hippocampal CA3 pyramidal neurons after synaptic activity

		Na	Mg	P	Cl	K	Ca	
		(mmol/kg dry weight) Mean ± SEM						
	n							Median
Mitochondria								
Control	45	25 ± 3	24 ± 1	378 ± 17	26 ± 3	299 ± 16	1.1 ± 0.4	1.2
1 sec	58	23 ± 2	21 ± 2	261 ± 9	30 ± 2	189 ± 10	7.9 ± 1.8	2.4*
30 sec	137	103 ± 6**	35 ± 2**	417 ± 10	65 ± 5**	302 ± 10	17.4 ± 2.7	5.8***#
180 sec	50	21 ± 2	24 ± 1	370 ± 8	17 ± 1	304 ± 9	0.7 ± 0.5	0.8
ER†								
Control	73	76 ± 7	41 ± 2	465 ± 12	61 ± 6	567 ± 16	5.8 ± 1.1	3.9
1 sec	36	60 ± 5	26 ± 2	323 ± 14	65 ± 5	388 ± 35	7.6 ± 1.5	5.5
30 sec	96	197 ± 12**	40 ± 2	483 ± 14	79 ± 6*	466 ± 16	20.1 ± 3.0	12.6***#
Responsive ER	(39%)						41.3 ± 5.9	30.7***###
Unresponsive ER	(61%)						6.2 ± 0.7	6.4
180 sec	48	73 ± 8	28 ± 1	379 ± 11	62 ± 4	473 ± 19	14.0 ± 1.3	11.6***
Responsive ER	(42%)						23.2 ± 1.4	22.3***
Unresponsive ER	(58%)						7.4 ± 0.7	7.2
Cytoplasm								
Control	53	78 ± 8	51 ± 5	354 ± 19	48 ± 3	745 ± 44	0.8 ± 0.9	0.7
1 sec	30	144 ± 28	47 ± 5	385 ± 30	120 ± 12**	689 ± 58	6.1 ± 1.5	5.1**
30 sec	143	251 ± 13**	54 ± 2	421 ± 10	81 ± 6**	643 ± 20	5.6 ± 0.6	4.5***
180 sec	48	70 ± 6	45 ± 3	294 ± 17	46 ± 4	687 ± 31	4.1 ± 1.2	4.4*

Data for all elements are given as mean ± SEM, where the SEM is based on the number of individual measurements, *n*, in that group. Because the distribution of Ca, but not other elements, in most compartments after stimulation is not normal (Kolmogorov–Smirnov test), Ca concentrations also are given as medians.

Values significantly higher than control or 1 sec data are indicated by the symbols * or $^{\#}p < 0.05$, $^{**}p < 0.01$, and *** or $^{\#\#\#}p < 0.001$, respectively. For all elements except Ca, significance was determined by one-way ANOVA, followed by the Dunnett test for multiple comparisons (vs control). For Ca, significance was tested by Kruskal–Wallis rank ANOVA with Dunn's test for nonparametric unbalanced data. Sampling strategy and data analysis are described further in Materials and Methods.

†Morphologically defined ER consisted of two populations, termed "responsive" and "unresponsive," with different Ca uptake activities; they can be differentiated only after ER Ca accumulation (see also Pozzo-Miller et al., 1997).

same experimental group; therefore, data from individual cultures (control, $n = 4$; 1 sec, $n = 3$; 30 sec, $n = 5$; 180 sec, $n = 3$) were pooled to calculate group means and medians. For all elements except Ca, statistical differences among experimental groups were determined using one-way ANOVA, followed by the Dunnett's test for multiple comparisons (vs controls). Because much of the critical data for Ca was not distributed normally, as determined by the Kolmogorov–Smirnov normality test, Ca concentrations are given as both means and medians in Table 1. Similarly, and for the sake of clarity, convenience, and consistency, Ca concentrations are presented throughout the text as both means and medians. However, Ca data in all figures are medians. Statistical differences between Ca concentrations in various experimental groups were determined using the Kruskal–Wallis nonparametric ANOVA with Dunn's test for multiple comparisons of unbalanced data. Analysis was performed by means of InStat software (GraphPad Software, San Diego, CA).

RESULTS

Afferent synaptic stimulation evokes calcium uptake by dendritic mitochondria

CA3 pyramidal neurons in hippocampal slice cultures respond to high-frequency stimulation of afferent mossy fibers with micromolar elevations in dendritic $[Ca^{2+}]_i$ that reach a maximum in ~1 sec and decay to baseline in <20 sec (Pozzo-Miller et al., 1993; Petrozzino et al., 1995). To investigate correlated changes in the concentration and distribution of intracellular total Ca, we rapidly froze slice cultures at 1 or 30 sec after a single 1 sec/50 Hz tetanus. This afferent stimulation, identical to the "single train" stimulus used in previous studies (Pozzo-Miller et al., 1997), depolarizes most of the dendrites on most of the CA3 neurons in slice culture (for acute slice experiments, see Jaffe et al., 1992; Magee et al., 1995; Spruston et al., 1995; Johnston et al., 1996; Helmchen, 1999). Subsequently, concentrations of total Ca, as well as Na, Mg, P, Cl, and K within the three principal subcellular compartments of CA3 proximal apical dendrites, namely, mitochondria, ER, and cytoplasm (Fig. 1), were measured by EPMA of freeze-dried cryosections prepared from frozen slice cultures. Because the aim of the present experiments was to characterize the Ca^{2+} buffering behavior of the various dendritic compartments after Ca^{2+} influx, measurements were performed only in those dendrites that responded to the stimulus train as indicated by the characteristic elemental changes known to accompany depolarization-induced Ca^{2+} influx.

The results revealed a rapid, graded, and reversible elevation in the total Ca concentration within dendritic mitochondria ($[Ca]_{mito}$). Afferent tetanic stimulation induced a significant elevation of $[Ca]_{mito}$ at both 1 sec [to 7.9 mmol/kg dry weight (mean); 2.4 mmol/kg (median)] and 30 sec [to 17.4 mmol/kg (mean); 5.8 mmol/kg (median)] after synaptic activation, compared with the characteristically low $[Ca]_{mito}$ [1.1 mmol/kg (mean); 1.2 mmol/kg (median)] in dendrites of control cultures that were grown, mounted, and frozen identically but received only low-frequency test stimuli (Table 1; Fig. 2*A*, *right panel*). (Because measurements of Ca concentrations were not distributed normally under conditions of Ca^{2+} uptake, as discussed below, Ca concentrations are given throughout the text as both means and medians; see Materials and Methods for details.) As an indication of how robust mitochondrial Ca accumulation could be, individual local measurements of $[Ca]_{mito}$ ranged as high as 60.0 mmol/kg at 1 sec and 220 mmol/kg at 30 sec. To place these observations in a biochemical perspective, the mean concentra-

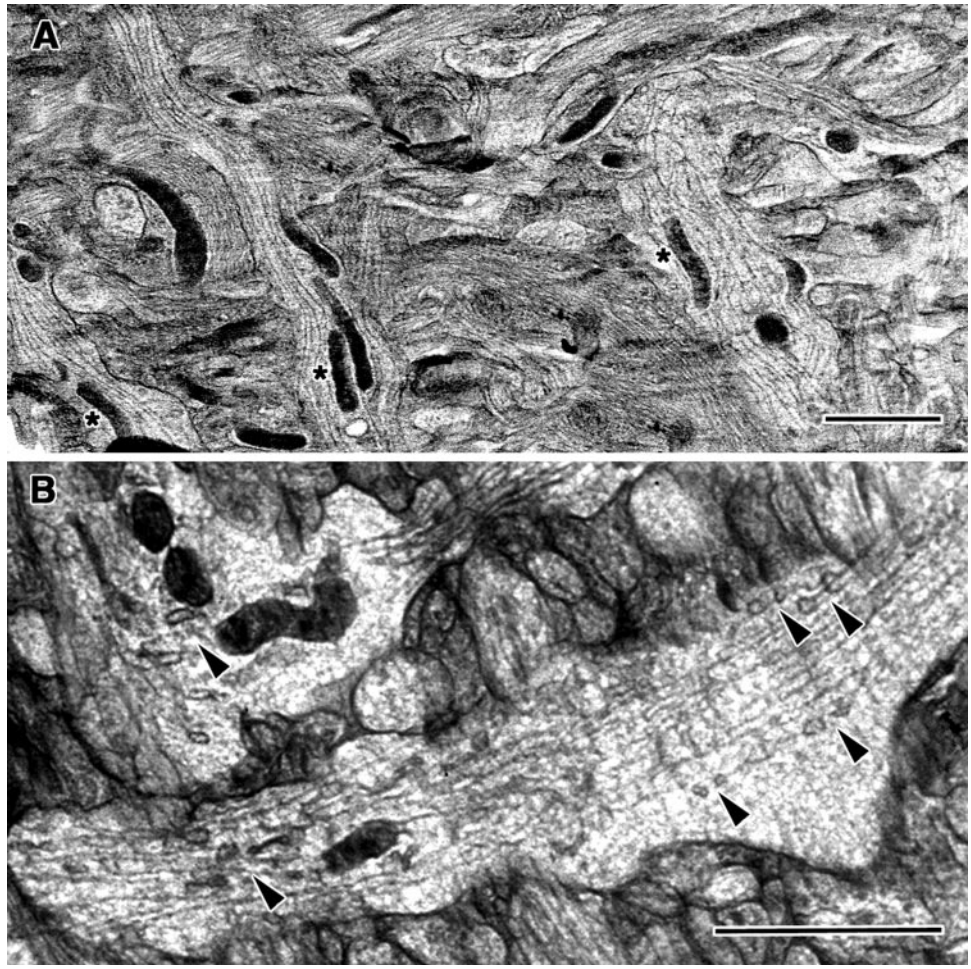

Figure 1. Ultrastructural organization of proximal dendrites in CA3 hippocampal neurons. Shown are representative digital transmission electron micrographs of freeze-dried cryosections prepared from rapidly frozen hippocampal slice cultures, illustrating the subcellular structure of proximal dendritic compartments and demonstrating that the three compartments targeted for EPMA (ER, mitochondria, and cytoplasm) are readily identifiable. Images were recorded using standard low-dose techniques in a LEO 912 Omega cryoanalytical electron microscope at −170°C by means of a ProScan slow-scan CCD camera (1024 × 1024). Survey view (*A*) shows the general appearance of the proximal dendritic field of CA3 neuropil in unstained cryosections from slice cultures. Three primary dendrites (*asterisks*) course across the field; cytoplasm, characterized by longitudinal bundles of microtubules, and elongated mitochondria (adjacent to *asterisks*) are evident. At higher magnification (*B*) both mitochondria and ER [essentially the only intracellular organelles present in proximal apical dendrites at the distance that was sampled (50–100 μm from the soma)] are apparent. The latter is seen as a network of smooth-surfaced cisterns, often in clusters (*arrowheads*). Together, the ER, mitochondria, and cytosol comprise essentially all of the dendritic volume while also including all important components of the Ca^{2+} regulatory system. Scale bars, 1 μm.

tions given above are equivalent (assuming that mitochondria are 75% protein by weight) to increases from resting levels of ~1.5 nmol/mg protein to ~10.5 and ~23.2 nmol/mg protein, respectively. This elevation of mitochondrial Ca is transient, as indicated by the finding, consistent with previous observations (Pozzo-Miller et al., 1997) that under identical conditions $[Ca]_{mito}$ had recovered completely 3 min after stimulation.

Among other intracellular elements, only sodium was elevated dramatically as a result of the afferent tetanus. Total Na elevations occurred not just in mitochondria but in all three dendritic compartments and were especially large at 30 sec (Table 1). Comparable changes previously were observed in CA3 dendrites in the same preparation after strong stimulation with four successive tetani and were attributed to the expected enhanced activity of Na^+ channels and Na^+/Ca^{2+} exchangers (Pozzo-Miller et al., 1997). Stimulus-induced Cl increases also were detected; as expected, these were smaller and appeared to progress sequentially from cytosol to mitochondria, consistent with counter-ion flow through the cell. Like Ca, the Na and Cl elevations were completely reversible, returning to prestimulus levels in all compartments by 3 min after the tetanus (Table 1).

Calcium sequestration in dendritic ER is slower than in mitochondria but persists longer

The ER of responsive dendrites (as described in the previous section) also exhibited elevated levels of total Ca ($[Ca]_{ER}$) at 30 sec after stimulation, but, in contrast to mitochondria, not at 1 sec (Table 1; Fig. 2*A*, *middle panel*). $[Ca]_{ER}$ was elevated only in a responsive subset of ER cisterns, defined as those in which $[Ca]_{ER}$ exceeded 15 mmol/kg dry weight. This population, ~40% of analyzed cisterns with a mean $[Ca]_{ER}$ of 41.3 mmol/kg dry weight (median, 30.7 mmol/kg), was qualitatively and quantitatively similar to the subset of Ca-sequestering ER previously characterized in these slice cultures (Pozzo-Miller et al., 1997). The remaining ~60% of smooth membrane elements within the same responsive dendrites evidently do not accumulate Ca, because they belong to a normally distributed population with a mean $[Ca]_{ER}$ of ~6 mmol/kg, statistically indistinguishable from control ER (Table 1). These cisterns are very likely also elements of the true endoplasmic reticulum, because other smooth-membraned cisterns or vesicles are quite rare at the sampled level of primary hippocampal dendrites. We note that if the nonaccumulating ER pool were contaminated adventitiously by non-ER elements, this would have the effect of deflating the estimate of the responsive ER fraction but would not affect quantitative comparisons of Ca accumulation between organelles.

At 3 min after stimulation $[Ca]_{ER}$ was still elevated (Table 1; Fig. 2*A*, *middle panel*), indicating that Ca^{2+} uptake by the ER continued, or was at least sustained (depending on the magnitude and rate of Ca^{2+} release from ER), for several minutes beyond the termination of Ca^{2+} entry. The ratio of responsive/nonresponsive cisterns essentially was unchanged, arguing against late recruitment to the responsive pool.

The fractional water and dry mass contents of mitochondria, ER, and cytoplasm differ substantially. Consequently, to compare

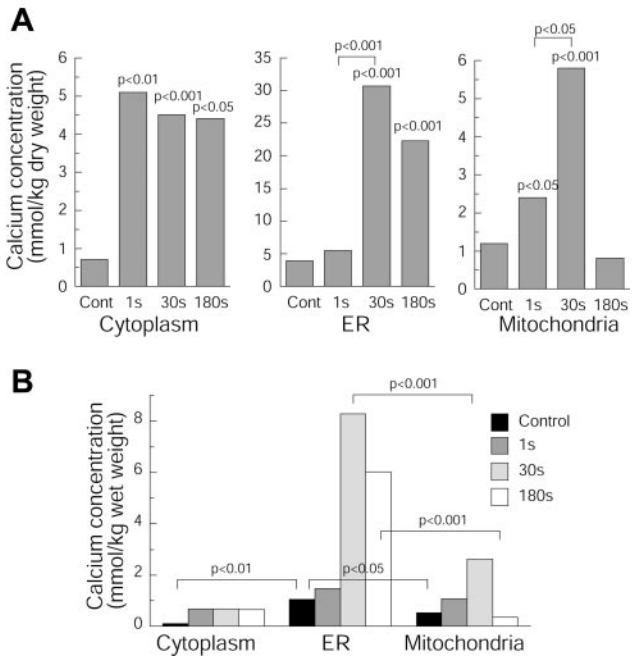

Figure 2. Calcium accumulation in dendritic compartments of CA3 hippocampal neurons. Comparison of calcium concentrations at different time points after synaptic stimulation in three dendritic compartments. In certain instances data were not distributed normally; therefore, all results are given as medians. In *A*, data are in primary units of mmol/kg dry weight. In *B*, Ca concentrations have been converted to mmol/kg wet weight (as described in Materials and Methods) to facilitate quantitative comparisons of Ca concentrations between compartments. Uncertainties introduced by this conversion are discussed in Results. Statistical significance (*p* values) relative to corresponding resting Ca concentrations is given above the *bars*; other significant differences are indicated by *bracketed pairs*. Statistical tests are described in Materials and Methods. *A*, At 1 sec after afferent synaptic stimulation $[Ca]_{mito}$ and $[Ca]_{cyto}$, but not $[Ca]_{ER}$, were elevated compared with resting levels. By 30 sec after stimulation Ca concentrations were elevated in all three compartments. (For ER, only data from the subpopulation that actively sequesters Ca in responsive dendrites, as presented in Table 1 and discussed in Results, are included.) By 180 sec after stimulation only $[Ca]_{mito}$ had recovered. Note the different *y*-axes. *B*, At rest, ER Ca levels are significantly higher than those in mitochondria and cytosol (compare *black bars*). The ER also contains by far the highest Ca concentrations at 30 and 180 sec (compare *light gray* and *white bars*), but not at 1 sec (*dark gray bars*).

the distribution of Ca between compartments, it is necessary to convert EPMA-derived Ca concentrations to hydration-compensated units such as mmol/kg wet weight (which is also approximately equivalent to mmol/l hydrated cell volume). Median data in Figure 2*B* have been converted as described in Materials and Methods. Although this conversion inevitably introduces additional uncertainties attributable, for example, to errors in the estimation of dry mass fractions for each compartment, it serves to factor out the effects of compartmental mass differences so as to convey a realistic sense of the quantitative differences in the amounts of sequestered Ca in different organelles. $[Ca]_{ER}$ in control slices was much higher on a wet-weight basis than $[Ca]_{mito}$ or cytoplasmic total Ca ($[Ca]_{cyto}$) (Fig. 2*B*), indicating that under basal conditions the ER is the most powerful Ca^{2+} buffer. This observation is also consistent with a role for dendritic ER as a releasable Ca^{2+} store (Seymour-Laurent and Barish, 1995; Pozzo-Miller et al., 1996; Garaschuk et al., 1997; Emptage et al., 1999; Nakamura et al., 1999; Rae et al., 2000). At 30 sec after tetanic stimulation, when both ER and mitochondria are accumulating Ca avidly, $[Ca]_{ER}$ is substantially larger than $[Ca]_{mito}$ (Fig. 2*B*). The difference is even greater at 3 min after stimulation, at which time $[Ca]_{ER}$ is still elevated significantly, but $[Ca]_{mito}$ has recovered completely. $[Ca]_{ER}$ was not significantly different from the control at 1 sec post-tetanus, indicating a delay of at least 1 sec before net ER Ca^{2+} uptake begins.

$[Ca]_{cyto}$ in CA3 dendrites was elevated maximally within 1 sec of stimulation (Table 1; Fig. 2*A*, *left panel*). Although the absolute increase in the cytoplasmic Ca concentration is modest, ~5 mmol/kg dry weight, and much less than in ER or mitochondria, the cytoplasmic volume fraction is correspondingly larger than that of either organelle. Dendritic cytoplasm thus represents a significant Ca^{2+}-binding reservoir, approximately equivalent by amount to organelle sequestration (see also Pozzo-Miller et al., 2000).

Spatial heterogeneity of synaptically evoked mitochondrial Ca uptake

The values of $[Ca]_{mito}$ presented in Table 1 and Figure 2 are means or medians of measurements obtained with randomly placed probes (diameter, ~100 nm) in each mitochondria in a given dendrite and therefore represent spatially averaged concentrations. (A similar approach with ~50 nm diameter probes was used for measurements of $[Ca]_{ER}$.) This sampling strategy provides a reasonable estimate of spatially averaged $[Ca]_{mito}$ at the level of individual dendrites, although sequestered Ca is not distributed uniformly within, and perhaps among, individual mitochondria. Under resting conditions individual measurements of $[Ca]_{mito}$ were always low; as expected for brain mitochondria (Somlyo et al., 1985; Andrews et al., 1988). The distribution of these measurements is normal (Fig. 3*A*, *top*), with a tight dispersion consistent with that expected from statistical errors of EPMA analysis. After afferent fiber stimulation this distribution became skewed toward higher $[Ca]_{mito}$ by the emergence of a fraction of measurements with elevated $[Ca]_{mito}$ (Fig. 3*A*, *middle*, *bottom*). The most extreme members of this subset had exceedingly high $[Ca]_{mito}$, often >100 mmol/kg dry weight.

The skewed distribution of $[Ca]_{mito}$ after stimulation arises at least partly from spatial heterogeneity of accumulated Ca within individual mitochondria, as reflected in the widely dispersed values for single measurements within the same mitochondrion (Fig. 3*B*). The basis for this form of spatial heterogeneity lies in the chemical nature of mitochondrial Ca sequestration. We and others have reported evidence for the formation, in intact stimulated neurons, of discrete calcium- and phosphorus-rich complexes that are thought to reflect a reversible, high-capacity Ca storage mechanism (David, 1999; Pivovarova et al., 1999). In frog sympathetic neurons depolarized with high K^+ such complexes appear as one or more small (~10 nm) punctate inclusions within the mitochondrial matrix. A similar mechanism of mitochondrial Ca sequestration in CA3 dendrites would account for the frequency distributions of $[Ca]_{mito}$ observed here (Fig. 3*A*), in that some fraction of Ca-accumulating mitochondria nonetheless are expected to give low individual measurements of $[Ca]_{mito}$ because the local sites of Ca sequestration were missed by randomly placed probes. An additional level of heterogeneity, caused by variability among mitochondria, is also plausible and perhaps likely (see Discussion).

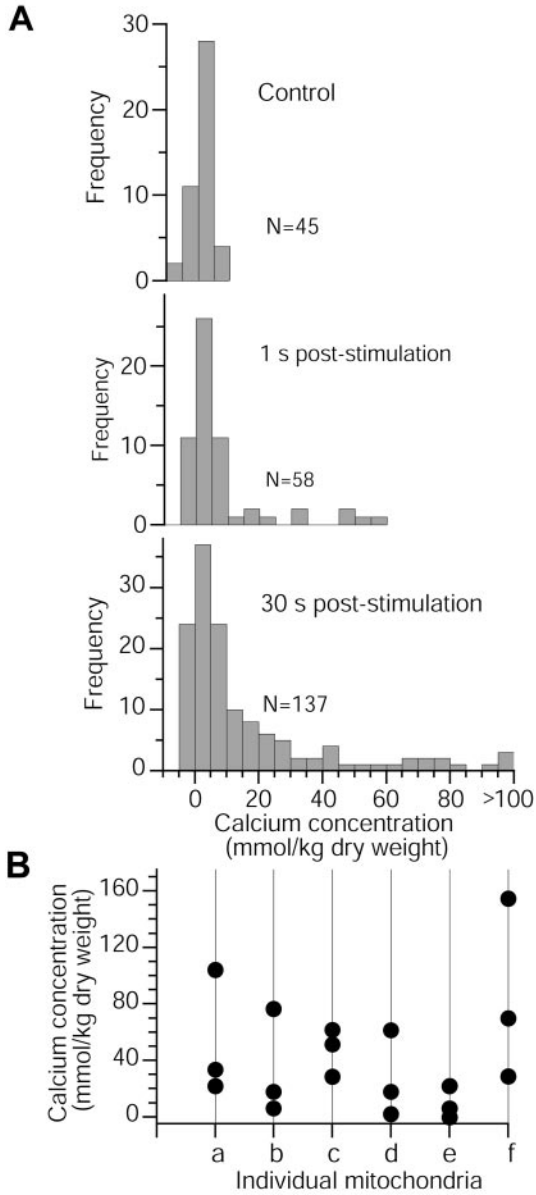

Figure 3. Heterogeneous distribution of $[Ca]_{mito}$ within individual mitochondria after synaptic stimulation. *A*, Mean $[Ca]_{mito}$ in resting dendrites is low, and the distribution of individual measurements is normal (*top panel*), as indicated by a good fit ($R^2 = 0.99$) to a single Gaussian with a width ($\sigma = 2.5$ mmol/kg dry weight) expected because of statistical uncertainties in EDX analysis. At 1 sec (*middle panel*) and 30 sec (*bottom panel*) the distribution becomes progressively skewed toward higher $[Ca]_{mito}$ as a result of a sequestration mechanism that concentrates Ca in small inclusions within the mitochondrial matrix. *B*, Distribution of single $[Ca]_{mito}$ measurements from six representative mitochondria with elevated Ca levels that were analyzed at three separate locations using a 100 nm probe. Large differences in $[Ca]_{mito}$ within each of these mitochondria reflect the heterogeneous distribution of calcium within individual mitochondria.

DISCUSSION

Mitochondria in a wide variety of cell types, including central pyramidal neurons (White and Reynolds, 1995; Wang and Thayer, 1996), accumulate Ca^{2+} after micromolar elevations in $[Ca^{2+}]_i$ (Pozzan and Rizzuto, 2000), but a significant role for dendritic mitochondrial Ca^{2+} uptake after synaptic activity-induced Ca^{2+} elevations has not been demonstrated. Most available data on mitochondrial Ca^{2+} transport in neurons come from somatic measurements and are therefore of uncertain relevance to dendritic Ca^{2+} signaling. The present experiments show that mitochondria in proximal dendrites of CA3 pyramidal neurons rapidly and transiently accumulate large amounts of Ca in the seconds after afferent fiber stimulation. Presumably, rapid Ca^{2+} uptake occurs because dendritic $[Ca^{2+}]_i$ reaches the supramicromolar levels (Petrozzino et al., 1995) consistent with strong activation of the mitochondrial uniporter (for isolated cardiac and liver mitochondria, EC_{50} ~10–20 μM; Gunter and Pfeiffer, 1990) and possibly the mitochondrial rapid uptake mode (RaM; Gunter et al., 2000). The Ca^{2+} uptake rate for dendritic mitochondria over the first second after synaptic stimulation is 9.0 ± 2.9 nmol/mg protein/sec (estimated from data in Table 1 as the difference between $[Ca]_{mito}$ at 1 sec and at rest). This value compares reasonably with the maximal velocity of the uniporter in isolated mitochondria (10–30 nmol/mg protein/sec; Gunter and Pfeiffer, 1990) as well as with Ca^{2+} uptake rates estimated in mitochondria of chromaffin cells (Babcock et al., 1997) and sympathetic neurons (Pivovarova et al., 1999). The large amounts of mitochondrially sequestered Ca found here are also consistent with data from physiologically stimulated nonexcitable cells (Montero et al., 2000).

Dendritic mitochondria still retain a significant Ca load 30 sec after stimulation (Fig. 2), well after $[Ca^{2+}]_i$ essentially has returned to prestimulus levels. By this time the net uptake rate has fallen dramatically, which is explained by the decreasing velocity of Ca^{2+} uptake as $[Ca^{2+}]_i$ declines and by the activation of mitochondrial Ca^{2+} extrusion mechanisms. The synaptically induced rise in $[Ca]_{mito}$ is completely reversible, as indicated by the observation that $[Ca]_{mito}$ has recovered to prestimulus levels 3 min after afferent stimulation (see also Pozzo-Miller et al., 1997). This implies a Ca^{2+} recovery half-time of 1–2 min, which is compatible with measured Ca^{2+} extrusion rates in other neuronal mitochondria (Colegrove et al., 2000) and also consistent with Ca^{2+} extrusion mainly via the Na^+/Ca^{2+} exchanger, the activity of which would, in turn, account for the elevated levels of mitochondrial Na^+ found here. Last, mitochondrial Ca^{2+} uptake after a single tetanic stimulus is consistent with similarly evoked changes in the mitochondria membrane potential in pyramidal dendrites (Bindokas et al., 1998), changes that presumably reflect mitochondrial Ca accumulation.

It should be mentioned that the dynamic pattern of elemental changes described here, namely, sequential or parallel elevation and recovery of cytoplasmic and organelle Ca and Na, has been observed in other neuronal systems, for example in the somata of cerebellar granule cells (Kiedrowski et al., 1994) and sympathetic neurons (Pivovarova et al., 1999) after strong K^+ depolarization, and appears to be a characteristic, physiologically normal consequence of Ca^{2+} entry and/or clearance mechanisms. In contrast to injurious stimuli, e.g., anoxia (Taylor et al., 1999) or high concentrations of glutamate (Kiedrowski et al., 1994), which evoke very large elevations of cytoplasmic Ca and Na, tetanus-evoked elevations of these elements are much smaller and completely reversible (Table 1) (Pozzo-Miller et al., 1997) and can be triggered repeatedly and reproducibly. Accumulating evidence suggests that Na^+ spikes or transients in pyramidal dendrites may subserve important functions such as triggering Ca^{2+} entry (Jaffe et al., 1992; Spruston et al., 1995; Johnston et al., 1996) or even acting as an independent signaling pathway (Callaway and Ross, 1997; Rose and Konnerth, 2001). Similarly, large cytosolic Na^+ elevations appear to be an important component of transmitter release mechanisms in presynaptic terminals (Zhong et al., 2001).

So far we have evaluated mitochondrial Ca^{2+} uptake on the basis of averaged measurements of $[Ca]_{mito}$ at random locations within individual mitochondria, but this approach is oversimplified because the actual spatial distribution of accumulated Ca is clearly heterogeneous. One major factor underlying this heterogeneity is the punctate distribution of sequestered Ca within the matrix of individual mitochondria. This distribution is a reflection of a major mechanism of Ca^{2+} buffering and sequestration that, as described above (Fig. 3), gives a skewed distribution of individual measurements of $[Ca]_{mito}$. This occurrence obscures higher levels of heterogeneity such as intermitochondrial variations that might reflect variability in mitochondrial energetics (Buckman and Reynolds, 2001) or spatial distribution (Collins et al., 2002) or in local $[Ca^{2+}]_i$ levels. In sympathetic neurons (Pivovarova et al., 1999), as well as in other excitable and nonexcitable cells (Montero et al., 2000; Collins et al., 2002), there is evidence for differences in Ca^{2+} uptake between individual mitochondria responding to the same stimulus in the same cell. These differences appear to depend at least partly on proximity to a local Ca^{2+} source. For mitochondria in dendrites of pyramidal neurons a similar heterogeneous response would be consistent with the skewed $[Ca]_{mito}$ distribution, but evidence that this occurs is masked because the intramitochondrial Ca-rich inclusions affect the frequency distributions in the same way as would intermitochondrial heterogeneity. If, in fact, there are differences in $[Ca]_{mito}$ between mitochondria, this well may reflect proximity to Ca^{2+} channels of the dendritic plasma membrane, a situation for which there is evidence in sympathetic neurons (Pivovarova et al., 1999) and secretory cells (Tse et al., 1997). Spatially resolved $[Ca]_{mito}$ measurements, i.e., "calcium maps" (Meldolesi and Grohovaz, 2001), will be necessary to address this issue.

Present results confirm and extend our previous observation that, within dendrites that have responded to synaptic stimulation with an increase in $[Ca^{2+}]_i$, a specific subset of ER has a profound capacity for accumulating and storing calcium. Figure 4 compares the magnitude and time courses of mitochondrial and ER Ca^{2+} uptake and release. It illustrates the fact that, in both dendritic organelles, the evoked Ca load persists well after decay of the Ca^{2+} transient, but the ER Ca load is particularly long-lived; previously published observations (Pozzo-Miller et al., 1997) indicate that Ca-accumulating ER may sustain their Ca load for longer than 15 min. Another interesting new finding is that ER Ca^{2+} uptake appears to be delayed for at least 1 sec relative to the cytosolic Ca^{2+} transient and to the onset of mitochondrial Ca^{2+} uptake. This may reflect the relative Ca^{2+} dependencies of the uptake mechanisms, i.e., the uniporter and RaM versus sarcoplasmic/endoplasmic reticulum Ca^{2+}-ATPase (SERCA) pumps in the ER. Alternatively, it may indicate release from Ca stores, which is known to be evoked in CA3 pyramidal neurons by mossy fiber activation (Pozzo-Miller et al., 1996; Yeckel et al., 1999). The role of releasable stores in dendritic Ca^{2+} signaling is an area of active investigation. Several recent studies indicate that Ca^{2+} release from ryanodine-sensitive and/or IP_3-sensitive internal stores may be a significant mechanism for signal amplification and/or modulation in both dendrites and spines of hippocampal neurons (Seymour-Laurent and Barish, 1995; Pozzo-Miller et al., 1996; Garaschuk et al., 1997; Emptage et al., 1999; Nakamura et al., 1999, 2000; Yeckel et al., 1999; Rae et al., 2000; Kapur et al., 2001). In the present case, because the ER reloads and even overloads during later stages of net Ca accumulation, dendritic ER may act first as a Ca^{2+} source to amplify the original Ca^{2+} signal and later switch into a buffering mode. We have demonstrated recently such a switchover in the caffeine/ryanodine-sensitive Ca stores of sympathetic neurons (Albrecht et al., 2001; Hongpaisan et al., 2001).

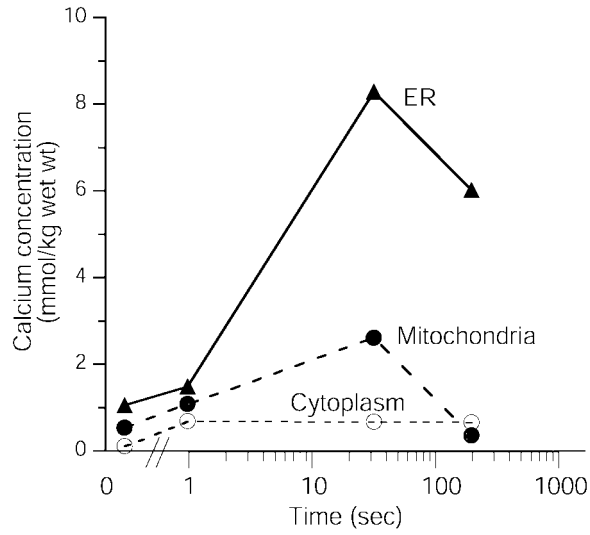

Figure 4. Calcium dynamics in dendritic compartments after synaptic stimulation. Time courses for $[Ca]_{cyto}$ (*open circles*), $[Ca]_{mito}$ (*filled circles*), and $[Ca]_{ER}$ (*filled triangles*; responsive subset only at 30 and 180 sec) illustrate complementary temporal relationship for activity-dependent Ca^{2+} uptake and release by dendritic mitochondria and ER. These organelles appear to transport Ca^{2+} within distinct, possibly cooperative, time domains. For example, $[Ca]_{mito}$ increases earlier and declines faster than $[Ca]_{ER}$, which remained elevated for >10 min. Data are given as medians. Note the log scale on the *abscissa*.

Much recent work supports the idea that interactions between the Ca^{2+} transport mechanisms of ER and mitochondria determine how these organelles cooperate or compete to modulate cytoplasmic Ca^{2+} signals (Hajnoczky et al., 2000; Rizzuto et al., 2000). Transfer of Ca^{2+} from the ER to the mitochondrion is the general (but not universal; Hoth et al., 1997; Hongpaisan et al., 2001) direction of transport. As noted previously (Pozzo-Miller et al., 2000), comparison of the time courses of Ca^{2+} transport by dendritic mitochondria and ER shows that these organelles accumulate and release Ca^{2+} in distinct and complementary time domains (Fig. 4), raising the possibility of a cooperative relationship. Mutual interdependence also is suggested by experiments showing that thapsigargin inhibition of ER Ca^{2+} uptake greatly enhances mitochondrial Ca^{2+} uptake (Pozzo-Miller et al., 1997). It is not clear whether the interactions underlying ER/mitochondria coupling are direct, as proposed for nonexcitable cells (Rizzuto et al., 1998), or mediated via changes in global $[Ca^{2+}]_i$. In either case any Ca "shuttling" at longer times in CA3 dendrites must be from mitochondria to ER, because dendritic ER retains its Ca load much longer than do mitochondria. Although the details of such interactions remain to be fully understood, it is clear that the ER and mitochondria of pyramidal dendrites play a fundamental role in shaping dendritic calcium signals during synaptically driven neuronal activity.

REFERENCES

Albrecht MA, Colegrove SL, Hongpaisan J, Pivovarova NB, Andrews SB, Friel DD (2001) Multiple modes of calcium-induced calcium release in sympathetic neurons I: attenuation of endoplasmic reticulum Ca^{2+} accumulation at low $[Ca^{2+}]_i$ during weak depolarization. J Gen Physiol 118:83–100.

Andrews SB, Leapman RD, Landis DM, Reese TS (1988) Activity-

dependent accumulation of calcium in Purkinje cell dendritic spines. Proc Natl Acad Sci USA 85:1682–1685.
Babcock DF, Hille B (1998) Mitochondrial oversight of cellular Ca^{2+} signaling. Curr Opin Neurobiol 8:398–404.
Babcock DF, Herrington J, Goodwin PC, Park YB, Hille B (1997) Mitochondrial participation in the intracellular Ca^{2+} network. J Cell Biol 136:833–844.
Berridge MJ (1998) Neuronal calcium signaling. Neuron 21:13–26.
Bindokas VP, Lee CC, Colmers WF, Miller RJ (1998) Changes in mitochondrial function resulting from synaptic activity in the rat hippocampal slice. J Neurosci 18:4570–4587.
Brocard JB, Tassetto M, Reynolds IJ (2001) Quantitative evaluation of mitochondrial calcium content in rat cortical neurones following a glutamate stimulus. J Physiol (Lond) 531:793–805.
Buchanan RA, Leapman RD, O'Connell MF, Reese TS, Andrews SB (1993) Quantitative scanning transmission electron microscopy of ultrathin cryosections: subcellular organelles in rapidly frozen liver and cerebellar cortex. J Struct Biol 110:244–255.
Buckman JF, Reynolds IJ (2001) Spontaneous changes in mitochondrial membrane potential in cultured neurons. J Neurosci 21:5054–5065.
Budd SL, Nicholls DG (1996) Mitochondria, calcium regulation, and acute glutamate excitotoxicity in cultured cerebellar granule cells. J Neurochem 67:2282–2291.
Callaway JC, Ross WN (1997) Spatial distribution of synaptically activated sodium concentration changes in cerebellar Purkinje neurons. J Neurophysiol 77:145–152.
Colegrove SL, Albrecht MA, Friel DD (2000) Quantitative analysis of mitochondrial Ca^{2+} uptake and release pathways in sympathetic neurons. Reconstruction of the recovery after depolarization-evoked $[Ca^{2+}]_i$ elevations. J Gen Physiol 115:371–388.
Collins TJ, Berridge MJ, Lipp P, Bootman MD (2002) Mitochondria are morphologically and functionally heterogeneous within cells. EMBO J 21:1616–1627.
David G (1999) Mitochondrial clearance of cytosolic Ca^{2+} in stimulated lizard motor nerve terminals proceeds without progressive elevation of mitochondrial matrix $[Ca^{2+}]$. J Neurosci 19:7495–7506.
David G, Barrett JN, Barrett EF (1998) Evidence that mitochondria buffer physiological Ca^{2+} loads in lizard motor nerve terminals. J Physiol (Lond) 509:59–65.
Duchen MR (1999) Contributions of mitochondria to animal physiology: from homeostatic sensor to calcium signaling and cell death. J Physiol (Lond) 516:1–17.
Emptage N, Bliss TV, Fine A (1999) Single synaptic events evoke NMDA receptor-mediated release of calcium from internal stores in hippocampal dendritic spines. Neuron 22:115–124.
Friel DD (2000) Mitochondria as regulators of stimulus-evoked calcium signals in neurons. Cell Calcium 28:307–316.
Friel DD, Tsien RW (1994) An FCCP-sensitive Ca^{2+} store in bullfrog sympathetic neurons and its participation in stimulus-evoked changes in $[Ca^{2+}]_i$. J Neurosci 14:4007–4024.
Gähwiler BH, Capogna M, Debanne D, McKinney RA, Thompson SM (1997) Organotypic slice cultures: a technique has come of age. Trends Neurosci 20:471–477.
Garaschuk O, Yaari Y, Konnerth A (1997) Release and sequestration of calcium by ryanodine-sensitive stores in rat hippocampal neurones. J Physiol (Lond) 502:13–30.
Gunter TE, Pfeiffer DR (1990) Mechanisms by which mitochondria transport calcium. Am J Physiol 258:C755–C786.
Gunter TE, Buntinas L, Sparagna G, Eliseev R, Gunter K (2000) Mitochondrial calcium transport: mechanisms and functions. Cell Calcium 28:285–296.
Hajnoczky G, Csordas G, Madesh M, Pacher P (2000) The machinery of local Ca^{2+} signaling between sarco-endoplasmic reticulum and mitochondria. J Physiol (Lond) 529:69–81.
Helmchen F (1999) Dendrites as biochemical compartments. In: Dendrites (Stuart G, Spruston N, Häusser M, eds), pp 161–192. New York: Oxford UP.
Helmchen F, Imoto K, Sakmann B (1996) Ca^{2+} buffering and action potential-evoked Ca^{2+} signaling in dendrites of pyramidal neurons. Biophys J 70:1069–1081.
Herrington J, Park YB, Babcock DF, Hille B (1996) Dominant role of mitochondria in clearance of large Ca^{2+} loads from rat adrenal chromaffin cells. Neuron 16:219–228.
Hongpaisan J, Pivovarova NB, Colegrove SL, Leapman RD, Friel DD, Andrews SB (2001) Multiple modes of calcium-induced calcium release in sympathetic neurons II: a $[Ca^{2+}]_i$- and location-dependent transition from endoplasmic reticulum Ca accumulation to net Ca release. J Gen Physiol 118:101–112.
Hoth M, Fanger CM, Lewis RS (1997) Mitochondrial regulation of store-operated calcium signaling in T lymphocytes. J Cell Biol 137:633–648.
Jaffe DB, Johnston D, Lasser-Ross N, Lisman JE, Miyakawa N, Ross WN (1992) The spread of Na^+ spikes determines the pattern of dendritic Ca^{2+} entry into hippocampal neurons. Nature 357:244–246.
Johnston D, Magee JC, Colbert CM, Christie BR (1996) Active properties of neuronal dendrites. Annu Rev Neurosci 19:165–186.
Kapur A, Yeckel M, Johnston D (2001) Hippocampal mossy fiber activity evokes Ca^{2+} release in CA3 pyramidal neurons via a metabotropic glutamate receptor pathway. Neuroscience 107:59–69.
Kiedrowski L, Brooker G, Costa E, Wroblewski JT (1994) Glutamate impairs neuronal calcium extrusion while reducing sodium gradient. Neuron 12:295–300.
Kitazawa T, Shuman H, Somlyo AP (1983) Quantitative electron probe analysis: problems and solutions. Ultramicroscopy 11:251–262.
Magee JC, Christofi G, Miyakawa H, Christie BC, Lasser-Ross N, Johnston D (1995) Subthreshold synaptic activation of voltage-gated Ca^{2+} channels mediates a localized Ca^{2+} influx into dendrites of hippocampal pyramidal neurons. J Neurophysiol 74:1335–1346.
Meldolesi J (2001) Rapidly exchanging Ca^{2+} stores in neurons: molecular, structural, and functional properties. Prog Neurobiol 65:309–338.
Meldolesi J, Grohovaz F (2001) Total calcium ultrastructure: advances in excitable cells. Cell Calcium 30:1–8.
Montero M, Alonso MT, Carnicero E, Cuchillo-Ibanez I, Albilos A, Garcia AG, Garcia-Sancho J, Alvarez J (2000) Chromaffin cell stimulation triggers fast millimolar mitochondrial Ca^{2+} transients that modulate secretion. Nat Cell Biol 2:57–61.
Nakamura T, Barbara JG, Nakamura K, Ross WN (1999) Synergistic release of Ca^{2+} from IP_3-sensitive stores evoked by synaptic activation of mGluRs paired with backpropagating action potentials. Neuron 24:727–737.
Nakamura T, Nakamura K, Lasser-Ross N, Barbara JG, Sandler VM, Ross WN (2000) Inositol 1,4,5-trisphosphate (IP_3)-mediated Ca^{2+} release evoked by metabotropic agonists and backpropagating action potentials in hippocampal CA1 pyramidal neurons. J Neurosci 20:8365–8376.
Nicholls DG, Budd SL (2000) Mitochondria and neuronal survival. Physiol Rev 80:315–360.
Peng Y-Y (1998) Effects of mitochondrion on calcium transients at intact presynaptic terminals depend on frequency of nerve firing. J Neurophysiol 80:186–195.
Petrozzino JJ, Pozzo-Miller LD, Connor JA (1995) Micromolar Ca^{2+} transients in dendritic spines of hippocampal pyramidal neurons in brain slice. Neuron 14:1223–1231.
Pivovarova NB, Hongpaisan J, Andrews SB, Friel DD (1999) Depolarization-induced mitochondrial Ca accumulation in sympathetic neurons: spatial and temporal characteristics. J Neurosci 19:6372–6384.
Pozzan T, Rizzuto R (2000) The renaissance of mitochondrial calcium transport. Eur J Biochem 267:5269–5273.
Pozzo-Miller LD, Petrozzino JJ, Mahanty NK, Connor JA (1993) Optical imaging of cytosolic calcium, electrophysiology, and ultrastructure in pyramidal neurons of organotypic slice cultures from rat hippocampus. NeuroImage 1:109–120.
Pozzo-Miller LD, Mahanty NK, Connor JA, Landis DMD (1994) Spontaneous pyramidal cell death in organotypic slice cultures from rat hippocampus is prevented by glutamate receptor antagonists. Neuroscience 63:471–487.
Pozzo-Miller LD, Petrozzino JJ, Golarai G, Connor JA (1996) Ca^{2+} release from intracellular stores induced by afferent stimulation of pyramidal neurons in hippocampal slice. J Neurophysiol 76:554–562.
Pozzo-Miller LD, Pivovarova NB, Leapman RD, Buchanan RA, Reese TS, Andrews SB (1997) Activity-dependent calcium sequestration in dendrites of hippocampal neurons in brain slices. J Neurosci 17:8729–8738.
Pozzo-Miller LD, Connor JA, Andrews SB (2000) Microheterogeneity of calcium signaling in dendrites. J Physiol (Lond) 525:53–61.
Rae MG, Martin DJ, Collingridge GL, Irving AJ (2000) Role of Ca^{2+} stores in metabotropic L-glutamate receptor-mediated supralinear Ca^{2+} signaling in rat hippocampal neurons. J Neurosci 20:8628–8636.
Regehr WG, Connor JA, Tank DW (1989) Optical imaging of calcium accumulation in hippocampal pyramidal cells during synaptic activation. Nature 341:533–536.
Reynolds IJ (1999) Mitochondrial membrane potential and the permeability transition in excitotoxicity. Ann NY Acad Sci 893:33–41.
Rizzuto R, Pinton P, Carrington W, Fay FS, Fogarty KE, Lifshitz LM, Tuft RA, Pozzan T (1998) Close contacts with the endoplasmic reticulum as determinants of mitochondrial Ca^{2+} responses. Science 280:1763–1766.
Rizzuto R, Bernardi P, Pozzan T (2000) Mitochondria as all-round players of the calcium game. J Physiol (Lond) 529[Pt 1]:37–47.
Roomans GM, Von Euler A (1996) X-ray microanalysis in cell biology and cell pathology. Cell Biol Int 20:103–109.
Rose CR, Konnerth A (2001) NMDA receptor-mediated Na^+ signals in spines and dendrites. J Neurosci 21:4207–4214.
Seymour-Laurent KJ, Barish ME (1995) Inositol 1,4,5-trisphosphate and ryanodine receptor distributions and patterns of acetylcholine- and caffeine-induced calcium release in cultured mouse hippocampal neurons. J Neurosci 15:2592–2608.

Somlyo AP (1985) Cell calcium measurement with electron probe and electron energy loss analysis. Cell Calcium 6:197–212.
Somlyo AP, Urbanics R, Vadasz G, Kovach AG, Somlyo AV (1985) Mitochondrial calcium and cellular electrolytes in brain cortex frozen *in situ*: electron probe analysis. Biochem Biophys Res Commun 132:1071–1078.
Spruston N, Schiller Y, Stuart G, Sakmann B (1995) Activity-dependent action potential invasion and calcium influx into hippocampal CA1 dendrites. Science 268:297–300.
Stoppini L, Buchs PA, Muller D (1991) A simple method for organotypic cultures of nervous tissue. J Neurosci Methods 37:173–182.
Stout AK, Raphael HM, Kanterewicz BI, Klann E, Reynolds IJ (1998) Glutamate-induced neuron death requires mitochondrial calcium uptake. Nat Neurosci 1:366–373.
Tang Y, Zucker RS (1997) Mitochondrial involvement in post-tetanic potentiation of synaptic transmission. Neuron 18:483–491.
Taylor CP, Weber ML, Gaughan CL, Lehning EJ, LoPachin RM (1999) Oxygen/glucose deprivation in hippocampal slices: altered intraneuronal elemental composition predicts structural and functional damage. J Neurosci 19:619–629.
Thayer SA, Miller RJ (1990) Regulation of the intracellular free calcium concentration in single rat dorsal root ganglion neurones *in vitro*. J Physiol (Lond) 425:85–115.
Tse FW, Tse A, Hille B, Horstmann H, Almers W (1997) Local Ca^{2+} release from internal stores controls exocytosis in pituitary gonadotrophs. Neuron 18:121–132.
Wang GJ, Thayer SA (1996) Sequestration of glutamate-induced Ca^{2+} loads by mitochondria in cultured rat hippocampal neurons. J Neurophysiol 76:1611–1621.
White RJ, Reynolds IJ (1995) Mitochondria and Na^{+}/Ca^{2+} exchange buffer glutamate-induced calcium loads in cultured cortical neurons. J Neurosci 15:1318–1328.
Yeckel MF, Kapur A, Johnston D (1999) Multiple forms of LTP in hippocampal CA3 neurons use a common postsynaptic mechanism. Nat Neurosci 2:625–633.
Zenisek D, Matthews G (2000) The role of mitochondria in presynaptic calcium handling at a ribbon synapse. Neuron 25:229–237.
Zhong N, Beaumont V, Zucker RS (2001) Roles for mitochondrial and reverse mode Na^{+}/Ca^{2+} exchange and the plasmalemma Ca^{2+}-ATPase in post-tetanic potentiation at crayfish neuromuscular junctions. J Neurosci 21:9598–9607.